Available online at www.sciencedirect.com

ScienceDirect

Procedia CIRP 41 (2016) 765 – 770

www.elsevier.com/locate/procedia

48th CIRP Conference on MANUFACTURING SYSTEMS - CIRP CMS 2015

Analysis of camera calibration with respect to measurement accuracy

Oleksandr Semeniuta[a,*]

[a]*Gjøvik University College, Teknologivegen 22, 2815 Gjøvik, Norway*

* Corresponding author. Tel.: +47-968-30-780. *E-mail address:* oleksandr.semeniuta@hig.no

Abstract

Machine vision is used for applications such as automated inspection, process control and robot guidance, and is directly associated with increasing of manufacturing process flexibility. The presence of noise in image data affects robustness and accuracy of machine vision, which can be an obstacle for industrial applications. Accuracy depends on both feature detection, resulting in pixel values of the measures of interest, and vision systems calibration, which allows transforming pixel measurements into real-world coordinates. This paper analyzes the camera calibration process, and proposes a new method for camera calibration, based on numerical analysis of probability distributions of the calibration parameters and removal of outliers. The method can be used to improve accuracy and robustness of the vision systems calibration process.

Peer-review under responsibility of the scientific committee of 48th CIRP Conference on MANUFACTURING SYSTEMS - CIRP CMS 2015
Keywords: Industrial Automation; Machine vision; Camera calibration; Accuracy; Robustness

1. Introduction

Machine vision is a technological field aimed at application of computer vision for the industrial needs, including automatic inspection, process control, and robot guidance [1–4]. Because of streamlined development of industrial automation and robotics in the recent years, research within machine vision continues to grow. One of the advantages of vision systems as compared to other types of sensors lies in the ability of measuring a wide range of characteristics, to the big extent depending on the capabilities of vision software. Because of this inherent characteristic, industrial visions systems are often considered in connection with manufacturing flexibility and reconfigurability [5].

Any vision system starts its work by acquiring an image or a set of images from cameras or data storage devices. After the original images are loaded into computer memory, a vision system exerts a certain set of operations upon the them to obtain the final application-dependent information output in the end. The operations typically constitute the well-known image processing or computer vision algorithms, and their sequence resembles a pipeline, starting at the image acquisition phase and ending with obtaining the desired result.

In most of the industrial cases, one needs to obtain measurements from a vision system that are expressed in real-world coordinates. This requires transforming pixel measures into metric values. To perform such transformation, the knowledge of the appropriate rigid transformations and intrinsic parameters of the cameras need to be obtained. This information is determined during the system calibration process and depends on the particular configuration of the system. Typical configurations include rigidly mounted camera, camera mounted on the robot arm, and various stereo- and multi-camera configurations.

Regardless the system configuration, the process of camera calibration is essential for application of vision systems, and is focused on determining a set of camera intrinsic parameters. The latter describe pixel size, center of projection, principal length, and distortion characteristics.

Camera intrinsic parameters are unique for a particular camera, and specify the models of image formation process, namely pinhole camera model and distortion model. Finding these parameters is possible by matching interest points in a known 3D or planar object with their projection on the camera imager, identified by the appropriate feature detection procedure. Thus, because real-world coordinates of the interest points and the respective pixel coordinates are known, one can derive the unknown camera intrinsic parameters by closed-form solution and numerical optimization.

Because camera calibration techniques are inherently based on feature detection, they, as any other vision algorithms, are subjective to noise. In order for the vision measurements to be accurate enough, these parameters need to (1) be as close to their true value as possible, and (2) be robust to different image data inputs to the calibration procedure.

This paper presents a new method for calibration of machine vision system, based on numerical analysis of probability distri-

Peer-review under responsibility of the scientific committee of 48th CIRP Conference on MANUFACTURING SYSTEMS - CIRP CMS 2015
doi:10.1016/j.procir.2015.12.108

butions of the camera intrinsic parameters and removal of outliers. The method is therefore aimed at improving accuracy and robustness of the vision systems calibration process.

This paper is organized as follows. Section 2 overviews the problem of vision system calibration, including pinhole camera model, various camera calibration techniques and methods for assessment and improvement of accuracy. Sections 3 and 4 provide description and validation of the proposed method respectively. Section 5 concludes the work.

2. Theory and related work

2.1. Pinhole camera model

In order to transform pixel measurements into real-world coordinates, one requires a model capturing the process of image formation. This model is ought to map 3D points in the world to 2D points in the image. To serve this role, a pihnole camera model is used, which describes a camera made as a chamber with a tiny hole on the front. This hole, also denoted as a pinhole aperture, defines an optical center of the camera. A light ray that passes thought the aperture, projects onto the back wall of the chamber, which is called an image plane, resulting in an inverted projection of the observed scene. A distance f from the image plane to the optical center is called principal distance or, in some literature, focal length.

A pinhole camera model uses two coordinate frames:

1. Camera coordinate frame $(x_{camera}, y_{camera}, z_{camera})$, located in the optical center, with z_{camera} axis perpendicular to the image plane;
2. Image coordinate frame (x_{screen}, y_{screen}), located in the top left corner of the image plane with x_{screen} and y_{screen} representing pixel rows and columns respectively.

Because $(x_{camera}, y_{camera}, z_{camera})$ is a right-hand frame, and image plane is inverted, x_{camera} and y_{camera} axes are directed opposite to the respective x_{screen} and y_{screen} axes. To simplify the calculations, the image plane is virtually positioned in front of the pinhole plane.

Detailed derivation of the pinhole camera model based on the abovementioned considerations is provided in [1,6]. The final model transforming a point in real-world coordinates to the image plane pixel coordinates can be presented as follows:

$$x_{screen} = f_x \frac{x_{camera}}{z_{camera}} + c_x \tag{1}$$

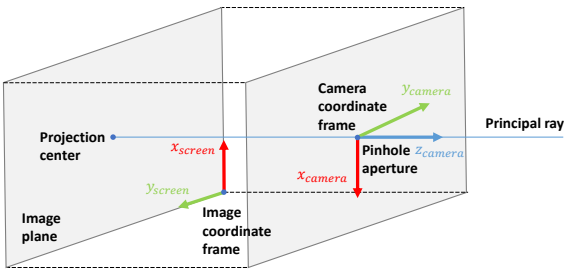

Fig. 1. Coordinate frames in the pinhole camera model.

$$y_{screen} = f_y \frac{y_{camera}}{z_{camera}} + c_y \tag{2}$$

Typically, the physical position of a point is known not in the camera coordinate frame, but in the world coordinate frame. The latter is related to the former by the respective rigid transformation $\mathbf{T}^{\mathbf{camera}}_{\mathbf{world}}$. Having this in mind, it is possible to express the pinhole camera model in matrix form as follows:

$$\begin{bmatrix} x_{screen} \cdot w \\ y_{screen} \cdot w \\ w \end{bmatrix} = \begin{bmatrix} f_x & 0 & c_x & 0 \\ 0 & f_y & c_y & 0 \\ 0 & 0 & 1 & 0 \end{bmatrix} \begin{bmatrix} r_{11} & r_{12} & r_{13} & d_1 \\ r_{21} & r_{22} & r_{23} & d_2 \\ r_{31} & r_{32} & r_{33} & d_3 \\ 0 & 0 & 0 & 1 \end{bmatrix} \begin{bmatrix} x_{world} \\ y_{world} \\ z_{world} \\ 1 \end{bmatrix} \tag{3}$$

Or, for short:

$$\begin{bmatrix} x_{screen} \cdot w \\ y_{screen} \cdot w \\ w \end{bmatrix} = \mathbf{M}\mathbf{T}^{\mathbf{camera}}_{\mathbf{world}} \begin{bmatrix} x_{world} \\ y_{world} \\ z_{world} \\ 1 \end{bmatrix} \tag{4}$$

The goals of camera calibration, therefore, is to determine camera intrinsic parameters (embodied in camera matrix $\mathbf{M}$) and camera extrinsic parameters (embodied in rigid transformation $\mathbf{T}^{\mathbf{camera}}_{\mathbf{world}}$).

2.2. Camera calibration

The general principle of camera calibration lies in finding the correspondence between a sufficiently large number of known 3D points and their projections in the image [1]. The known points are provided by the calibration object containing features that have known coordinates and are easily identifiable by vision algorithms. A calibration object may be different depending on one of the following calibration techniques: [7]

1. 3D reference-object based calibration: a precisely manufactured 3D object (typically, consisting of three perpendicular planes) is used [8,9].
2. 2D plane-based calibration: multiple views of the same planar object are processed [10,11].
3. 1D line-based calibration: three or more collinear points (e.g. string of balls) are used [7].
4. Self-calibration: no calibration object is required; intrinsic and extrinsic parameters are recovered from feature points correspondences after moving camera in a static scene.

Because manufacturing of a custom 3D object is costly, planar objects make calibration process more flexible. Self-calibration is reported to be less reliable comparing to the object-based calibration techniques [10]. 1D line-based calibration is only useful in specific use cases, such as computing relative geometry in multi-camera systems [7]. This paper will therefore focus on 2D plane-based calibration, and more specifically the method proposed by Zhang [10] and Sturm et al. [11], and implemented in OpenCV.

In OpenCV, the abovementioned method is organized as follows. The camera takes m images of the planar calibration object from different views. For each view i, a homography matrix $\mathbf{H_i}$ is computed based on two sets of points: (1) real-world coordinates of the target points in the world coordinate frame, and

(2) their projected pixel values determined with the appropriate feature detection technique. Then, a closed-form solution to equation 5 is found.

$$\mathbf{Vb} = 0 \tag{5}$$

where $\mathbf{V}$ represents $2m \times 6$ matrix obtained from the homography matrices and the constraints imposed by the orthonormality of the rotation vectors, and $\mathbf{b}$ is a 6×1 vector formed from the expressions based on the unknown camera intrinsic parameters.

The camera matrix $\mathbf{M}$ derived from $\mathbf{b}$, the extrinsic parameters for each view $\mathbf{T}^{\mathbf{camera}}_{\mathbf{world}}$ are computed having $\mathbf{H_i}$ and $\mathbf{M}$.

After the closed-form solution to (5) is found, the camera matrix $\mathbf{M}$ is refined by maximum likelihood estimation minimizing the projection error.

In the OpenCV implementation, distortion coefficients are computed using the method proposed in [12], and, based on them, the values of $\mathbf{M}$ are reestimated [6].

2.3. Increasing accuracy of camera calibration

"International vocabulary of metrology" defines measurement *accuracy* as "closeness of agreement between a measured quantity value and a true quantity value of a measurand" [13, p. 21]. The document also notes that accuracy is not a quantity expressed as a numerical value but an attribute of a measurement: a measurement is said to be more accurate if it results in a smaller measurement error. Accuracy, according to [14], is a matter of calibration, and "can be determined only by repeatedly measuring a standard that has a known true value" [14, p. 294].

Measurement *precision* is defined as "closeness of agreement between indications or measured quantity values obtained by replicate measurements on the same or similar objects under specified conditions" [13, p. 22]. As [14] notes, precision is "the ability of a measurement process to repeat its results" [14, p. 292], i.e. the more precise the process, the less variability around its mean it has. Typical measures of precision are standard deviation, variance and coefficient of variation [13].

To ensure more accurate results of the calibration algorithm, a number of requirements has to be met. The view of planar calibration target shall not parallel in two or more calibration images. For better estimation of the camera distortion, the calibration target shall appear in all four corners of the image and cover as much exterior orientations as possible [1]. Also, according to [10], the best results would be obtained providing more than 10 calibration object views and orientation angle near 45°.

In [15], three calibration techniques, developed by Tsai, Heikkilä and Zhang, are evaluated with respect to factors influencing camera calibration accuracy. The methods of Tsai [8] and Heikkilä [9] are examples of 3D reference-object based calibration, whereas Zhang's method [10], also described above, uses several views of a planar calibration object. Four measures of accuracy were assessed in [15] with respect to noise, quantity of training data, and distortion model:

1. Error of distorted pixel coordinates.
2. Error of undistorted pixel coordinates.
3. Distance with respect to the optical ray.
4. Normalized calibration error.

As it is shown in [15], the plane-based calibration method is most sensitive in terms of accuracy comparing to the 3D object-based methods.

In [16], accuracy and robustness of Zhang's calibration algorithm was improved by removing outlier feature points in each image used for calibration. A feature point is considered an outlier if its projection error is unacceptably high. This may be caused by image noise, uneven illumination, contamination of the camera or the object surface, or performance of the feature detector implementation. The outliers are removed in two stages: (1) threshold selection, excluding the points with the largest reprojection error, and (2) RANSAC algorithm, finishing the outliers removal.

In [17], the problem of inaccurate identification of feature points during calibration process is tackled. Specifically, the difficulty arises in distorted non-fronto parallel images. To refine the feature points coordinates, the authors propose an iterative approach, in which the original images are undistorted and unprojected onto fronto-parallel plane, and then the camera parameters are recomputed. This process is repeated until convergence.

In [18], the Zhang's calibration method is supplemented with additional optimization routine. The latter minimizes 3D distance between the point of intersection of calibration plane with optical ray and known feature point in camera coordinate frame.

In [19], statistical and neural networks methods were applied for increasing accuracy of distortion coefficient calibration.

3. Method

3.1. True intrinsics estimation

Different sets of images used for camera calibration lead to different intrinsic parameters of the same camera. It is assumed that this process has normal error distribution, and therefore, if calibration is performed n times, it would be possible to recover the natural mean of values of the camera intrinsic parameters. These mean values are dubbed in this paper as *true intrinsics*.

Let I denote a large set of images with different calibration object views, in all of which the features were correctly detected. If the total size of I is N, then $I = \{im_1, im_2, ...im_N\}$.

Let S denote a powerset of randomly drawn subsets of I, each of size m. Thus, $S = \{s_1, s_2, ...s_n\}$ such that $s_k \in I^m$.

The maximal number of unique m-length combinations from N objects, given $m \leq N$, is computed as follows:

$$C_N^m = \frac{N!}{m!(N-m)!} \tag{6}$$

With the increase of size N of set I, the number of possible m-length combinations grows significantly. Therefore, if N is sufficiently large, it is possible to generate the required number of *unique* subsets from I.

As [10] notes, the most accurate calibration results are obtained when $m \geq 10$. Let $m = 15$ given the size of the large set $N = 20$. In this case, $C_N^m = 15504$. If one takes $n = 200$, it is possible to assure that each s_k is unique within S.

The proposed algorithm for recovering *true intrinsics* is presented as follows:

1. Acquire a set $I_{original}$ of original images of the calibration pattern in different orientations.
2. In each image $im_k \in I_{original}$ detect the calibration object features. Those images where feature detection was successful, belong to a new set $I \subseteq I_{original}$ having length N.
3. With given subset size m and number of unique subsets n, check whether $n \leq C_N^m$. If the latter expression holds true, proceed. Otherwise, terminate.
4. Generate n subsets from I of size m: $S = \{s_1, s_2, ...s_n\}$.
5. Perform camera calibration for each image set $s_k \in S$.
6. Store calibration results in a data frame **D**, formed as a matrix $\mathbb{R}^{n\times 9}$ in which each row correspond to the camera intrinsic parameters $(f_x, f_y, c_x, c_y, k_1, k_2, p_1, p_2, k_3)$ obtained using s_k.
7. For each distribution of $p \in \{f_x, f_y, c_x, c_y, k_1, k_2, p_1, p_2, k_3\}$ (corresponding column in matrix **D**), compute mean μ_p and standard deviation σ_p by maximum likelihood estimation of a normal distribution.
8. From data frame **D** remove the rows in which value of at least one parameter $p \in \{f_x, f_y, c_x, c_y, k_1, k_2, p_1, p_2, k_3\}$ lies outside the range $[\mu_p - 3\sigma_p, \mu_p + 3\sigma_p]$. The new data frame is denoted as $\mathbf{D}^*$.
9. Reestimate mean μ_p and standard deviation σ_p given $\mathbf{D}^*$.
10. Repeat the previous two steps until there is no rows to exclude from $\mathbf{D}^*$ (i.e. for each row k, for $p \in \{f_x, f_y, c_x, c_y, k_1, k_2, p_1, p_2, k_3\}$, the following expression holds true: $(d_p^{(k)} \geq \mu_p - 3\sigma_p \wedge (d_p^{(k)} \leq \mu_p - 3\sigma_p))$.

3.2. Accuracy assessment

As it was noted above, the typical measure of camera calibration accuracy is a reprojection error, where, given intrinsic parameters $f_x, f_y, c_x, c_y, k_1, k_2, p_1, p_2, k_3$ and known extrinsic parameter of a view im_k, the known object points are projected onto the screen. Then, the root mean square (RMS) projection error is computed between real pixel coordinates (x_i, y_i) and the projected ones (x_i^{proj}, y_i^{proj}).

$$E_{reprojection} = \sqrt{\frac{1}{n_{features}} \sum_{i=1}^{n_{features}} [(x_i - x_i^{proj})^2 + (y_i - y_i^{proj})^2]} \quad (7)$$

RMS reprojection error is also used in Zhang's method [10] to optimize the intrinsic parameters. However, for a given image set s_k, the minimized RMS errors would be different. In this paper, the accuracy of the proposed algorithm is assessed compared to the accuracy of all other sets of intrinsic parameters (rows of data frame **D**).

Let $intr^{TI}$ are the camera intrinsic parameters obtained as the result of the method proposed in 3.1, and $intr^k$ are the camera intrinsic parameters obtained using the standard Zhang's method given the calibration imageset s_k. The accuracy of points reprojection shall be evaluated for each set of intrinsic parameters in $A = intr^{TI} \cup \{intr^k | s_k \in S\}$.

For each intrinsics set $intr_k \in A$, an RMS reprojection error can be computed given image im. To assess intrinsics accuracy with respect to image sets with varied camera orientations, mean RMS for each image set ought to be computed.

Table 1. Overview of data frame D and the estimated true intrinsics.

Parameter	Minimal value	Maximal value	TI value
f_x	3376.742	3423.129	3399.264
f_y	3375.722	3423.217	3397.573
c_x	543.549	583.711	565.067
c_y	302.567	404.123	350.885
k_1	-0.226	-0.061	-0.146
k_2	-10.652	2.731	-2.803
p_1	-0.007	0.000	-0.004
p_2	-0.001	0.001	0.000
k_3	-58.128	277.285	66.072

3.3. Experimental setup

The calibration experiment is conducted upon a Prosilica GC1020, a 1024 × 768 resolution CCD camera with Gigabit Ethernet interface with the attached Pentax C1814-M 16 mm lens.

To calibrate the camera using Zhang's algorithm, a chessboard having 7 × 5 corners pattern, with square size 30.0 mm is used.

Image acquisition is performed using Scorpion vision software. The used calibration routine: OpenCV 3.0.0.

4. Results

To perform true intrinsics estimation, a calibration image set $I_{original}$ is acquired. From $I \subseteq I_{original}$, $n = 200$ subsets of size $m = 18$ are generated and used for camera calibration with the standard OpenCV routine. The obtained distributions of intrinsic parameters are presented in figures 2 – 10. Having the distributions, true intrinsics estimation (3.1) is performed. On figures 2 – 10, a red vertical line corresponds to the obtained value of an intrinsic parameter, and green vertical lines specify the respective 6σ range $[\mu_p - 3\sigma_p, \mu_p - 3\sigma_p]$.

Table 1 presents the minimal and maximal value of each intrinsic parameter given the original data frame **D**, and the corresponding true intrinsic value.

To assess accuracy of the camera intrinsic parameters in $A = intr^{TI} \cup \{intr^k | s_k \in S\}$, a test image set $I_{original}^{(test)}$ is used, acquired using the same camera and the same calibration object. From $I^{test} \subseteq I_{original}^{(test)}$, $n^{(test)} = 50$ subsets of size $m^{(test)} = 25$ are generated, forming set $S^{(test)}$. Furthermore, for $(intr_i, s_j) \in A \times S^{(test)}$,

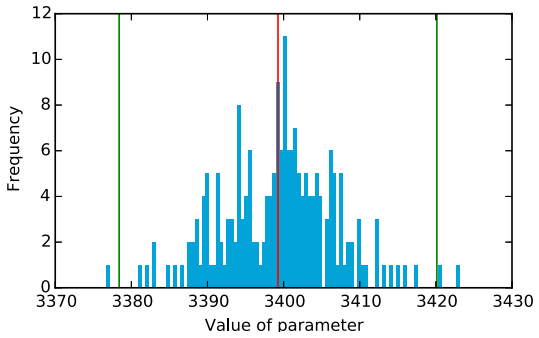

Fig. 2. f_x distribution histogram.

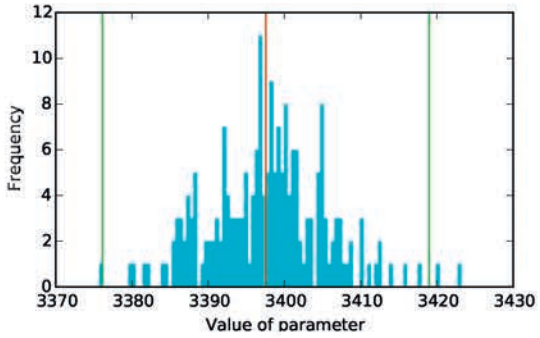

Fig. 3. f_y distribution histogram.

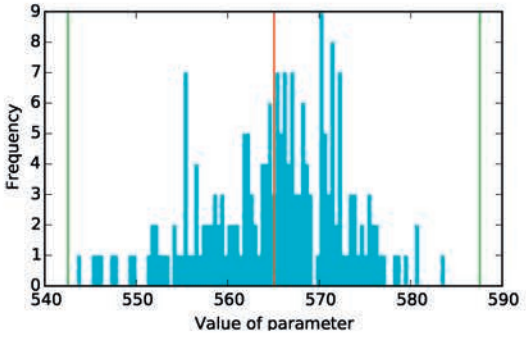

Fig. 4. c_x distribution histogram.

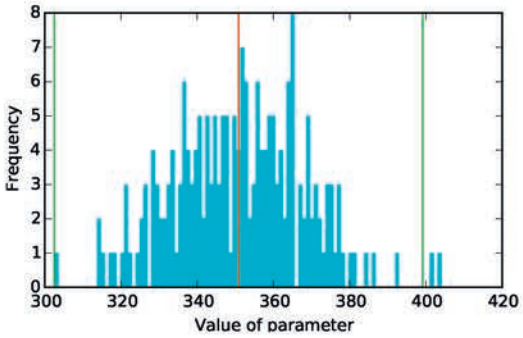

Fig. 5. c_y distribution histogram.

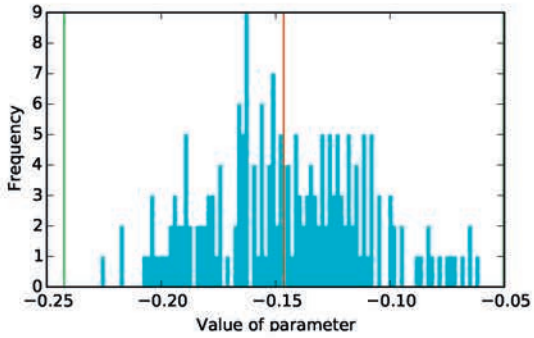

Fig. 6. k_1 distribution histogram.

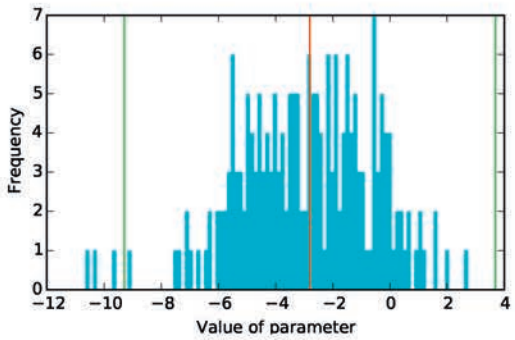

Fig. 7. k_2 distribution histogram.

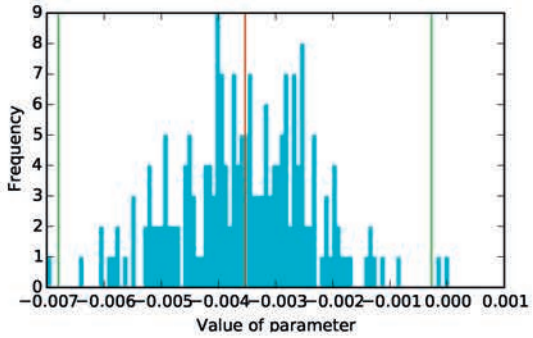

Fig. 8. p_1 distribution histogram.

the mean reprojection error is computed.

As table 2 shows, all the intrinsic parameters in A result in a similar reprojection error. Intrinsics $intr^{TI}$ result in smaller error comparing to the average one. However, among $n = 200$ original intrinsics, there exist 18 sets that result in smaller error value as compared to $intr^{TI}$. Therefore, in 91% of cases, the proposed method improves the accuracy of camera calibration.

Table 2. Accuracy assessment.

Measure	Value
Mean RMS among all $(intr_i, im_j) \in A \times S^{(test)}$	0.2576
Mean RMS given $intr^{TI}$ for all $im_k \in S^{(test)}$	0.2561
Number of the intrinsic sets yielding smaller mean RMS than $intr^{TI}$ for all $im_k \in S^{(test)}$	18/200

5. Conclusion and further work

In this paper a method of camera calibration was presented in which the natural central tendencies of the intrinsic parameters are computed by maximum likelihood estimation based from the respective probability distributions. The method utilizes outliers elimination using threshold selection based on natural 6σ distribution spread. The proposed method provides a robust solution to camera calibration in the sense that, for each intrinsic parameter, natural mean and standard deviation, rather than a fixed value, is returned.

Given different sets of camera intrinsic parameters obtained during calibration of the same camera using the different image sets, the proposed method results in higher accuracy in 91%

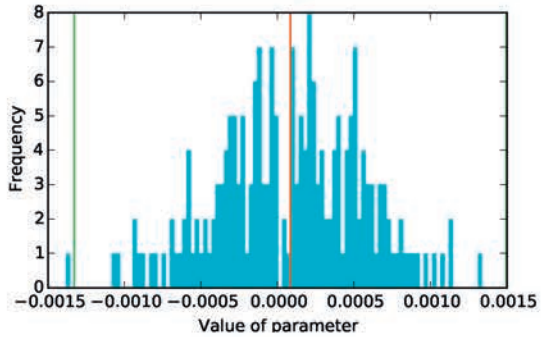

Fig. 9. p_2 distribution histogram.

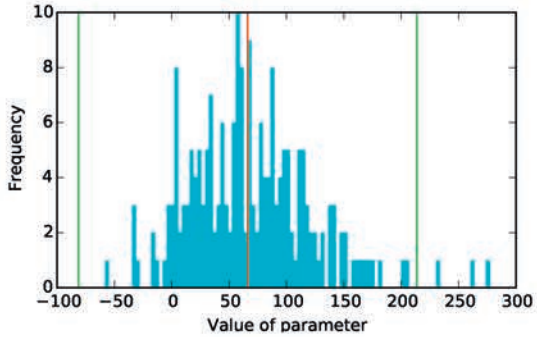

Fig. 10. k_3 distribution histogram.

cases. However, there exist 9% sets of intrinsic parameters that yield better accuracy comparing to the method proposed. Therefore, in the future an improvement of the presented algorithm shall be done. A possible way to do it is to substitute maximum likelihood estimation with optimization-based selection process. In addition, to be used in practice, computation efficiency of the algorithm need to be improved, and estimation of accuracy shall also be performed in 3D space.

6. Acknowledgments

This research is funded by the Norwegian Research Council. The author would like to express his gratitude to Sebastian Dransfeld and Ådne Solhaug Linnerud from SINTEF Raufoss Manufacturing AS for sharing their ideas and technical experience.

References

[1] Steger, C, Ulrich, M, Wiedemann, C. Machine Vision Algorithms and Applications. Wiley-VCH Textbook; Wiley-VCH; 2007. ISBN 9783527407347.

[2] Malamas, EN, Petrakis, EGM, Zervakis, M, Petit, L, Legat, JD. A survey on industrial vision systems, applications and tools. Image and Vision Computing 2003;21(2):171–188. doi:http://dx.doi.org/10.1016/S0262-8856(02)00152-X.

[3] Sonka, M, Hlavac, V, Boyle, R. Image Processing, Analysis, and Machine Vision. Thomson-Engineering; 2007. ISBN 049508252X.

[4] Golnabi, H, Asadpour, A. Design and application of industrial machine vision systems. Robotics and Computer-Integrated Manufacturing 2007;23(6):630–637. doi:http://dx.doi.org/10.1016/j.rcim.2007.02.005.

[5] Rosati, G, Faccio, M, Carli, A, Rossi, A. Convenience analysis and validation of a fully flexible assembly system. In: Emerging Technologies & Factory Automation (ETFA), 2011 IEEE 16th Conference on. ISBN 1946-0740; 2011, p. 1–8.

[6] Bradski, G, Kaehler, A. Learning OpenCV: Computer Vision with the OpenCV Library. O'Reilly Media; 2008. ISBN 9780596554040.

[7] Zhang, Z. Camera calibration with one-dimensional objects. Pattern Analysis and Machine Intelligence, IEEE Transactions on 2004;26(7):892–899.

[8] Tsai, R. A versatile camera calibration technique for high-accuracy 3d machine vision metrology using off-the-shelf tv cameras and lenses. Robotics and Automation, IEEE Journal of 1987;3(4):323–344. doi:10.1109/JRA.1987.1087109.

[9] Heikkilä, J. Geometric camera calibration using circular control points. Pattern Analysis and Machine Intelligence, IEEE Transactions on 2000;22(10):1066–1077. doi:10.1109/34.879788.

[10] Zhang, Z. A flexible new technique for camera calibration. Pattern Analysis and Machine Intelligence, IEEE Transactions on 2000;22(11):1330–1334.

[11] Sturm, PF, Maybank, SJ. On plane-based camera calibration: A general algorithm, singularities, applications. In: Computer Vision and Pattern Recognition, 1999. IEEE Computer Society Conference on.; vol. 1. ISBN 1063-6919; 1999, p. 437 Vol. 1.

[12] Brown, DC. Close-range camera calibration. Photogrammetric Engineering 1971;37(8):855–866.

[13] JCGM, . International vocabulary of metrology — basic and general concepts and associated terms (vim). 2008. URL: http://www.bipm.org/utils/common/documents/jcgm/JCGM_200_2008.pdf; accessed: 2014-03-11.

[14] Aikens, CH. Quality Inspired Management. The Key to Sustainability. Prentice Hall; 2011.

[15] Sun, W, Cooperstock, JR. An empirical evaluation of factors influencing camera calibration accuracy using three publicly available techniques. Machine Vision and Applications 2006;17(1):51–67. doi:10.1007/s00138-006-0014-6.

[16] Zhou, F, Cui, Y, Wang, Y, Liu, L, Gao, H. Accurate and robust estimation of camera parameters using ransac. Optics and Lasers in Engineering 2013;51(3):197–212. doi:10.1016/j.optlaseng.2012.10.012.

[17] Datta, A, Kim, J, Kanade, T. Accurate camera calibration using iterative refinement of control points. In: Computer Vision Workshops (ICCV Workshops), 2009 IEEE 12th International Conference on. ISBN 978-1-4244-4442-7; 2009, p. 1201–1208. doi:10.1109/ICCVW.2009.5457474.

[18] Zhou, F, Cui, Y, Peng, B, Wang, Y. A novel optimization method of camera parameters used for vision measurement. Optics and Laser Technology 2012;44(6):1840–1849. doi:10.1016/j.optlastec.2012.01.023.

[19] Smith, LN, Smith, ML. Automatic machine vision calibration using statistical and neural network methods. Image and Vision Computing 2005;23(10):887–899. doi:10.1016/j.imavis.2005.03.009.